SRD 2026

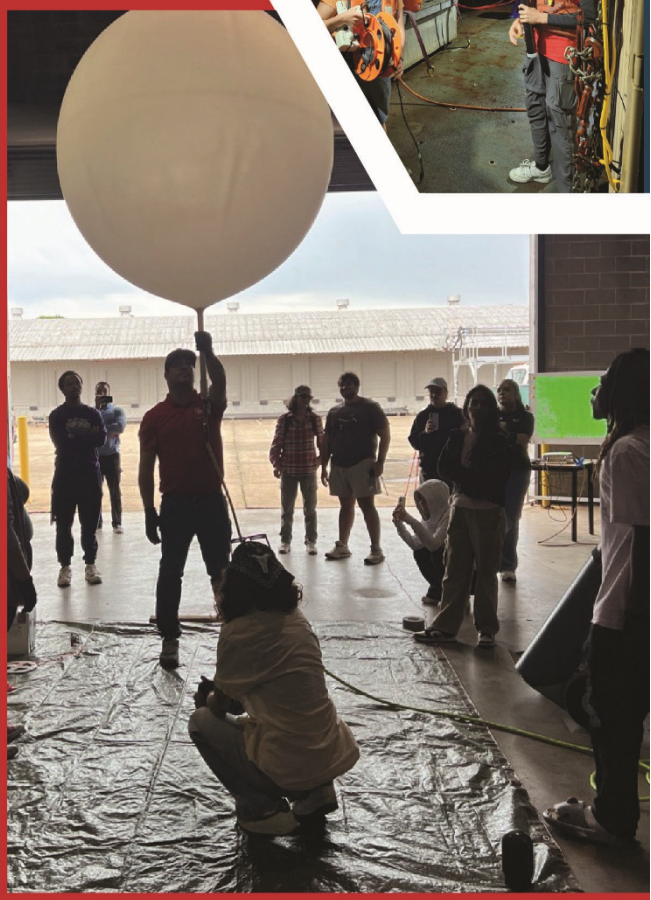

University of Houston

Earth and Atmospheric Sciences

39th Annual Student Research Conference

Friday, May 8th, 2026

Science and Research Building (SR1) 3507 Cullen Blvd., Houston, TX, 77204

Table of Contents

EAS Student Groups

American Association of Petroleum Geologists
aapg.wildcatters@gmail.com

American Meteorological Society (AMS)
uhstudentams@gmail.com

Association of Environmental and Engineering Geologists (AEG) and American Institute of Professional Geologists (AIPG)
AEGatUH2@gmail.com

Geological Society (GeoSociety)
geosocietyatuh@gmail.com

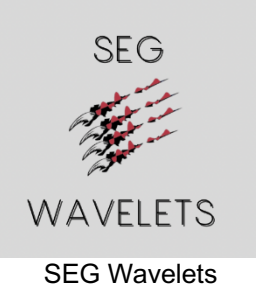

SEG Wavelets
segwavelets@gmail.com

See what these organizations are up to on the 2nd floor!

Schedule

Breakfast & Check In	8:30 – 9:30 a.m.
Talk Session 1	9:30 – 10:30 a.m.
Coffee Break	10:30 – 11:00 a.m.
Talk Session 2	11:00 – 12:00 p.m.
Lunch	12:00 – 1:00 p.m.
Poster Session	1:00 – 3:00 p.m.
Faculty Talk	3:00 – 3:25 p.m.
Awards Ceremony	3:25 – 4:45 p.m.
Group Photo	4:45 p.m.
Happy Hour	5:00 – 7:30 p.m.

Oral Presentations
SR1 Rooms 223 & 634

Poster Presentations
SR1 Floors 2, 3, and 4

Keynote Lecture
SR1 Room 634

Awards Ceremony
SR1 Room 634

Oral Presentations (SR1 223)

9:30 a.m.

Nabeel Muhammedy (MS)

Investigating the mechanical properties of iron-nickel meteorites for deep earth understanding and planetary defense

Iron-nickel meteorites are primary natural analogues for understanding the interiors of rocky planets, assessing planetary defense risks, and identifying resources for in-situ resource utilization (ISRU). However, the temperature-dependent elastic properties of these materials remain poorly constrained, creating uncertainties in models of core dynamics and the fragmentation of metal-rich (M-type) asteroids. This study investigates the mechanical properties of iron and stony-iron meteorites to link bulk seismic measurements to underlying microstructural controls. We combined contact ultrasonic measurements with multiscale characterization, including p-XRF, AFM, and Scanning Acoustic Microscopy (SAM), on samples with contrasting cooling histories. Preliminary results indicate that while shear moduli (μ) fall ~20 ± 5 percent below expected limits, bulk moduli (K) fall ~10 ± 5 percent below the theoretical Reuss lower bound. This suppression suggests that compressional deformation is preferentially accommodated by compliant phase boundaries and microcracks, rather than the intrinsic stiffness of the Fe-Ni alloy. Unlike S-type asteroids, where mechanical behaviour is dominated by porosity, the response of M-type bodies is governed by these complex metallic microstructures. Our results imply that iron meteorites fragment more efficiently than idealized metals due to enhanced stress wave attenuation at internal interfaces. These calibrated rock physics parameters will be integrated into the i-SALE hydrocode to refine impact and fragmentation models, supporting planetary defense initiatives such as the DART mission and future asteroid resource characterization.

9:45 a.m.

Oussama Romdhani (PhD)

Role of Turbulence Parametrization in Modulating Convective Organization over the Greater Houston Area

As global atmospheric models push toward higher resolutions, many, including E3SM, ICON, and SCREAM are increasingly operating in the so-called "grey zone" of model resolution, typically between 1 and 4 km. In this range, deep convection is partially resolved, traditional subgrid parameterizations may no longer be valid and the role of turbulence parameterization in shaping convective organization remains an open question. This study investigates the sensitivity of convective organization over the Houston Greater Area to horizontal mixing length, using the Weather Research and Forecasting (WRF) model. A suite of numerical experiments was conducted by systematically varying the horizontal mixing length in Smagorinsky turbulence scheme while keeping all other model physics and boundary conditions fixed. Analysis of cloud diameter distributions shows a pronounced shift toward larger cloud sizes with increasing horizontal mixing length, primarily due to a reduction in the frequency of small, isolated clouds. This suggests that stronger subgrid-scale turbulent mixing enhances the horizontal and vertical coupling, facilitating the organization of smaller convective elements into more coherent cloud structures. Notably, the largest convective systems (i.e. those typically associated with heavy precipitation) exhibited minimal sensitivity to the turbulence configuration, indicating a scale-dependent response where turbulence parameterization exerts control mainly on small-to-intermediate cloud sizes, but not on the largest systems. This underscores the importance of properly configuring subgrid-scale mixing parameters in convection-permitting simulations, particularly over complex urban regions like Houston.

10:00 a.m.

Johanna Villagomez (PhD)

GulfNet: Large-scale nodal seismic deployment along the Texas-Louisiana Coast

Offshore Gulf of Mexico (GOM) in Texas and Louisiana has been proposed as a major site for geological carbon storage. However, there are many active geological fault systems in the region, such as the Corsair, Clemente-Tomas and Frio Fault Zones. It is critical to study the dynamics of these faults and potential seismic events associated with any fault movement. Currently, there are few seismic stations near the coast to monitor these activities. To fill this observation gap, I have undertaken a massive field deployment effort. We have deployed more than 200 three component nodes along the Gulf Coast, spanning from Brownsville, TX to Grand Chenier, LA (~800 km), within 80 km of the coastline. Acquired data show clear surface wave dispersion curves of ambient noise correlations, demonstrating high data quality. This 19-month observation effort aims to establish a risk baseline in both seismic structure and seismicity for the GOM northern offshore region. Results on the sensitivity of our network, and a baseline seismicity catalog will be presented.

10:15 a.m.

Amberlee Enger (MS)

Using Isotope Geochemistry to Constrain Serpentinization and Carbonation of Modern Ocean Floor with Ancient Ties

Hydrothermal alteration of mafic minerals occurs when seawater percolates through seafloor basalts and peridotites at elevated temperatures (100-400°C), producing various hydrous minerals (Allen & Seyfried, 2004). The high abundance of olivine in peridotites leads to dramatically different hydrothermal reactions than for typical basaltic crust, generating high pH fluids, serpentine minerals, brucite, magnetite, and carbonates. Carbonate formation in natural serpentinite systems remains underexplored, hindering our understanding of modern geochemical cycles linking the atmosphere, oceans, and solid Earth. Given that serpentinization is conducive to the precipitation of carbonates, significant efforts are underway to optimize carbon sequestration efforts in ultramafic tailings (Stokreef et al., 2022). Major cation sources, reaction temperatures, and rates of both serpentinization and carbonation of peridotite-hosted carbonates remain uncertain.To address these questions, we have obtained 18 peridotite samples (~3 Ma) from Vavilov basin, Mediterranean Sea (IODP Expedition 402). Here, normal faulting has allowed for the infiltration of seawater and subsequent hydrothermal alteration (Sanfilippo et al., 2025). We will analyze major and trace element abundances and follow with $\delta^{44}Ca$, $\delta^{18}O$, and 87Sr/86Sr analyses on both silicate and carbonate phases from these samples. This combination of isotopic proxies allows us to evaluate the sources of Sr and Ca in the silicates and carbonates, the temperatures at which they likely equilibrated, and the reaction rates associated with carbonate precipitation. Additionally, Ca isotopes in peridotite-hosted carbonates are underexplored, so our data will likely have compounding implications for the use of $\delta^{44}Ca$ in tracing recycled carbonates in mantle-derived igneous rocks (Antonelli & Simon, 2020).

30 minute break

11:00 a.m.

Abe Okayli Masaryk (PhD)

Metamorphic fabric analysis with emphasis on spatial patterns

Interpretation of quartz crystallographic preferred orientation is expressed through c-axis opening angle and pole figures, enabling approximations of deformation conditions like temperature and strain conditions. The classical approach to fabric analysis is suffers from loss of information when spatial patterns are compressed in statistical bulk descriptors that do not inform about heterogeneity. This presentation will introduce a framework for metamorphic fabric analysis, focusing on quartz shear bands, that quantifies multi scale, intermittent patterns by treating micro structural data as an property that emerges from a dynamical system by treating fabric description with statistical physics. Such fabric descriptors are necessary to assist the development of a unified theory for deformation and metamorphism as processes that happen far from equilibrium (i.e. in a system with gradients).

11:15 a.m.

Karissa Vermillion (PhD)

Extinction of Late Cretaceous magmatism during shallow subduction and Oligocene initiation of the San Andreas transform margin and rifting in the western San Gabriel Mountains, California

The modern topographic expression of southern California is dominated by two major tectonic events. The Late Cretaceous transition from arc magmatism to shallow subduction and the Late Oligocene initiation of the San Andreas transform margin between the Pacific and North American plates. Evidence of both is preserved within the western San Gabriel Mountains (SGM). This includes accretion of trench-derived Pelona Schist during shallow subduction and deposition of >5 km of Oligocene–Miocene rift basin fill as the transform margin developed. Here, we investigate the impact of both events using 40Ar/39Ar thermochronology and coupled apatite U-Pb and fission-track thermochronology from SGM basement and basin-fill cobbles. 40Ar/39Ar thermal history results help better characterize the cooling histories of the upper and lower plates following Late Cretaceous arc cessation and accretion of the Pelona schist. The onset of rifting at ca. 25 Ma during the initial Pacific-North American plate interaction was caused by the subduction of the Mendocino Fracture Zone. Our apatite fission-track data show that rocks from the shallowest SGM crustal levels were eroded and preserved as cobbles in Late Oligocene–Miocene rift basins. A comparison between basement and lithologically equivalent cobbles indicate ~1.2–2.2 km of differential uplift during rifting. We propose a late Miocene marine incursion caused post-depositional burial and reheating to 80–60 ºC by 10 Ma. The modern SGM range was created by transpressional deformation since ca. 5 Ma due to the San Andreas restraining bend caused 2.3–5.3 km of uplift at 0.5–1.0 mm/a within the western SGM.

11:30 a.m.

Haini Wang (PhD)

Persistent Soil Drying in the Southwestern North America Over Recent Decades Attributed to Global Warming and Natural Oceanic Variability

Southwestern North America (SWNA) has experienced persistent drying since around 1979, especially in soil moisture. This drying has been attributed to different physical processes, but their relative contributions remain uncertain. To fill this gap, we built three models, including a multiple linear regression model, an eXtreme Gradient Boosting machine-learning model, and an empirical dynamical model with built-in causality, to simulate SWNA root-zone (0–1 m) soil-moisture anomalies observed during 1979–2022. In these models, global warming dominates the soil drying, explaining 39%–64% of the total trend. Phase transitions of the Pacific Decadal Oscillation and Atlantic Multidecadal Oscillation contribute ~11%–14% and ~9%–31%, respectively. Observational analyses indicate that the SWNA soil drying is mainly driven by the long-term decrease in precipitation due to enhanced atmospheric circulation divergence caused by changes in radiative forcing and ocean variability and is likely further exacerbated by increased vapor pressure deficit due to global warming.

11:45 a.m.

Rijul Dimri (PhD)

Operator Learning for PM2.5 Forecasting Using a Transport-Informed Machine Learning

Accurate short-term forecasting of PM2.5 concentrations is critical for air quality management and public health, yet existing approaches either depend on computationally intensive chemical transport models (CTMs) or lack physical interpretability. This study presents TransNet, a Graph Neural Network (GNN) that learns coupled Advection–Diffusion–Reaction (ADR) operators directly from monitoring station data, eliminating the need for CTM outputs. The model represents atmospheric transport processes as three learnable operators, advection via mass-conserving directional weights, diffusion via adaptive graph Laplacian operators, and reaction through pointwise multilayer perceptron, integrated using an operator splitting strategy that preserves numerical stability and physical consistency across forecast horizons. TransNet was trained on data from 170 AirKorea monitoring stations over 2018–2019, validated on 2020 data, and tested on 2021 data, forecasting PM2.5 concentrations across 72-hour lead times. At short-term horizons, TransNet achieves a Mean Absolute Error of 2.60 μg/m³ at +1h, representing a 39% improvement over AGATNet, a state-of-the-art bias-correction model, with corresponding improvements of 49% at +6h and 44% at +12h. Operator analysis reveals that the coupled advection–diffusion system is essential for short-term accuracy, with isolated configurations producing 72–73% error increases, while removing transport process increases errors by 153.5% at +1h. These findings demonstrate that physics-informed operator learning can provide computationally efficient, interpretable air quality forecasting, while substantially reducing operational costs. TransNet represents a step toward bridging purely data-driven models and full atmospheric simulation frameworks.

Lunch

Oral Presentations (SR1 634)

9:30 a.m.

Makenna Harris (MS)

Sedimentary charcoal records poorly preserve the stratigraphic signal of grassland fire as informed by the 2024 Windy Deuce Fire, Texas, Panhandle

Wildfires shape landscape evolution by removing vegetation and generating charcoal that may be transported and preserved in sedimentary archives. In steep, forested landscapes, post-fire rainfall commonly triggers rapid sediment and charcoal transport, producing distinct stratigraphic signals in downstream depositional environments. However, the transportation of charcoals, and preservation of wildfire signals in low-gradient, semi-arid grasslands remains poorly constrained. This study evaluates these processes following the 2024 Windy Deuce wildfire in the Texas Panhandle using sediment cores from Lake Meredith Reservoir, charcoal morphometric analyses and hydrologic modeling. Charcoal abundance and morphology were quantified across proximal, and distal depositional settings. Rainfall–runoff simulations were used to estimate rainfall intensity–duration thresholds required to generate surface flow capable of transporting charcoal under post-fire conditions. Charcoal presence in the cores lacks discrete enrichment associated with the recent fire. Modeled rainfall thresholds for charcoal transport (8–10 mm/hr over multiple hours) were rarely exceeded following wildfire, and no storms capable of generating sustained runoff occurred during the immediate post-fire period. Independent field observations indicate rapid post-fire vegetation regrowth, suggesting a short-lived window of hydrologic connectivity that further limited sediment and charcoal mobilization. Consequently, charcoal delivery to the reservoir occurs through low-energy fluvial transport rather than event-driven pulses capable of forming distinct stratigraphic layers. These results demonstrate that in low-slope, semi-arid grasslands, charcoal preservation depends on the timing of fire, rainfall, and recovery, rather than fire occurrence alone, and charcoal records from large grassland reservoirs may under-record wildfire activity when post-fire rainfall fails to exceed transport thresholds.

9:45 a.m.

Christina Raymond (MS)

Human-Engineered Waterways and Sediment Dynamics: A case study of Matagorda Bay and the Gulf Intracoastal Waterway

Matagorda Bay, Texas, is a productive, biodiverse estuarine system that supports local fisheries, ecotourism, and coastal communities. Ecosystem health depends on the balance of freshwater inflow and marine exchange. Along the Texas coast, the Gulf Intracoastal Waterway (GIWW), a ~40 m-wide, ~4 m-deep engineered navigation channel, runs parallel to the Gulf Coast and interacts with numerous embayments, including Matagorda Bay. Satellite imagery reveals visible sediment plumes entering the bay from GIWW outlets, suggesting that this human-built system may play an underappreciated role in sediment and freshwater delivery. To investigate the influence of the GIWW on sediment dynamics, we analyzed water samples and acoustic Doppler velocity (ADCP) measurements from the GIWW and the Colorado River diversion channel, historically considered the primary source of freshwater and sediment. Monthly water sampling shows that total suspended solids (TSS) concentrations at GIWW outlets are, on average, higher than those within and exiting the Colorado River. ADCP measurements show background velocities in the GIWW of 0.1 to 0.2 m/s, increasing to nearly 1 m/s during barge passages. These barge-induced velocity pulses coincide with increased turbidity, suggesting that vessel traffic repeatedly resuspends bed sediment that can then be transported through adjacent outlets into Matagorda Bay. These observations indicate that the GIWW functions as a human-driven sediment source, with vessel traffic acting as a mechanism for episodic sediment mobilization. This process has the potential to influence vertical sediment accretion, water clarity, and salinity structure, with implications for habitat stability, fisheries productivity,

and long-term resilience to sea-level rise. Ongoing work will integrate long-term monitoring and sediment core analyses to link modern sediment transport with historical accumulation patterns.

10:00 a.m.

Fnu Anshika (PhD)

Investigation of phthalate emissions from incense stick, scented candle and perfume through a chamber experiment

Phthalate exposure has been rampant with the growing use of these compounds in personal care and other plastic products. Phthalates have been associated with endocrine, neurological, and reproductive disorders resulting from their continuous release from plastic surfaces throughout their lifecycle. These endocrine disruptors are used in personal care products to increase their shelf life. This paper aims to identify phthalates and their concentration in three test materials, perfume, scented candles, and incense sticks, through a chamber experiment. This experiment aids in understanding phthalate emissions into air during the use of these materials in indoor environments. Sampling was performed using Tenax TA tubes, which were placed inside the glass chambers for 30 minutes while maintaining a positive flow rate using a mass flow controller and pump. The tubes capture gas-phase phthalates efficiently. The tubes were then further analyzed using TD-30 and GC/MS. Three phthalates, which were detected in the test materials, were dimethyl phthalate (DEP), dibutyl phthalate (DBP), and butyl benzyl phthalate (BBP). The phthalate concentration was found to be high in incense sticks, with DEP being the most prominent phthalate, followed by DBP. Scented candles had the high concentration of DBP, followed by BBP. A similar pattern was observed in perfumes. The high concentrations of these compounds detected in the test materials underscore growing concerns about the widespread use of phthalates in manufacturing of plastic products.

10:15 a.m.

Asmara Lehrmann (PhD)

Glacial geomorphology offshore Dotson Ice Shelf, Amundsen Sea, West Antarctica: new features from high-resolution AUV bathymetry

The seafloor offshore Dotson Ice Shelf, Amundsen Sea, West Antarctica, is characterized by geomorphic evidence of past glacial behavior recorded in bathymetric data from shipboard multibeam surveys. Here, we present a high-resolution autonomous underwater vehicle (AUV) multibeam bathymetric grid of an area offshore the eastern portion of Dotson Ice Shelf. The high-resolution data allows confirmation of earlier interpretations as well as the discovery of smaller scale and newly identified features. Features formed subglacially include drumlinoids (n=6), mega-scale glacial lineations (MSGL, n>800), and meltwater channels. Notably, there are 920 semi-regularly spaced channels on the flanks of the drumlinoids, perpendicular to glacial flow, that are <250 m long, <50 m wide, and <20 m deep. Regularly spaced channels perpendicular to drumlinoid axes have not previously been documented in either marine or terrestrial records. The most common channel cross-section geometry is V-shaped. The channels observed in this study include a subset with low-order branching. The branching features in this subset are V- or trapezoidal-shaped, but u-shaped cross sections only occur in the trunk channel. The channel form ratio and the dominance of V- or trapezoidal-shapes indicate that these channels could have formed by glacial meltwater erosion (e.g., Gales et al., 2013; Kirkham et al., 2019), or by turbidity current generation (e.g., Gales et al., 2013), or by a combination of these processes. Cross cutting five of the MSGL are linear divots that are in 820 m water, are 70-100 m long, 30-40 m wide, and 1-4 m deep. Though their formation mechanism is unclear, their geometry and relationship to the MSGL indicate they could be iceberg plough marks. If so, they are some of the deepest recorded iceberg plough marks in the Amundsen Sea and would indicate either an unusual overturning of a large tabular iceberg, or even thicker ice than previously thought.

30 minute break

11:00 a.m.

Rebekah Wells-Mourre (BS)

Integrating Multispectral UAV and Sentinel-2 Imagery to Quantify Suspended Sediment Dynamics and Its Ecological Impacts in Texas Coastal Bays

Trinity and Matagorda Bays are dynamic estuarine systems where water quality is strongly influenced by suspended sediment and freshwater inflow. Changes in suspended sediment can affect light penetration and dissolved oxygen (DO) conditions, which play an important role in overall ecosystem health. While these relationships are well recognized, capturing how they change across different spatial and temporal scales remains a challenge. To address this, this study integrates multispectral UAV imagery with a 10-year Sentinel-2 dataset to examine suspended sediment dynamics and turbidity in both bays. Monthly UAV surveys conducted from August 2024 to July 2025 provide high resolution reflectance data (green, red, red-edge, and near-infrared), which are used to calculate sediment indices like suspended sediment index (SSI), normalized difference turbidity index (NDTI), and bounded turbidity ratio (BTR). Sentinel-2 Level-2A imagery is used to extend the analysis across the full bay and over longer timescales using the same indices. Bathymetric data is also used to evaluate how depth and seafloor morphology influence sediment distribution. In addition, spatial datasets of seagrass and oyster reefs are used to assess potential ecological interactions with turbidity patterns. Trinity Bay is primarily river-dominated, while Matagorda Bay is more influenced by wind- and tidal-driven processes.

11:15 a.m.

Kenneth Shipper (PhD)

Modeling Source Rock UEP and Thermal Stress to Predict the Charge Fairway of the Guyana-Suriname Basin

The Guyana-Suriname basin has developed into one of the most prolific deepwater hydrocarbon provinces of the past decade. The “Golden Lane” play fairway has been established by more than 54 discoveries that extend from the southeastern Stabroek block of offshore Guyana into the adjacent Block 58 of offshore Suriname. The extent of this play fairway remains speculative, with a key risk being source rock maturation. I created a transient full-lithosphere 3D basin model integrating a dense 2D seismic grid, bottom-hole temperatures from 7 wells, and geochemical data from 15 wells to model source rock maturation from the easternmost maritime boundary of Trinidad and Tobago to the central Demerara Plateau. Geochemical analysis of source rocks across the shelf–slope shows Cretaceous intervals containing Organofacies B kerogen with organic carbon up to 6% and Hydrogen Index values between 200–600 mg HC/g TOC. This translates to a maximum ultimate expellable potential (UEP) of up to 126 mmboe/km² along the southeastern paleo shelf–slope. In the area of the Golden Lane fields, studied Cretaceous source rocks expel at least 3 mmbo/km² of expelled oil. Within the central play fairway, oil expulsion increases from 6 to 24 mmbo/km² to the northwest during the Cenomanian–Turonian interval, while values of ~4 mmbo/km² characterize the distal area of offshore Trinidad and Tobago. Expelled gas increases to 8 mmboe/km² near the maritime boundary between Guyana and Suriname and explains the lower gas-oil ratios (GOR) in the northwestern Golden Lane transitioning to higher GOR near the maritime boundary.

11:30 a.m.

Nima Khorshidian (PhD)

Non-Monotonic Effects of Urban Aerosols on Deep Convection: A WRF-Chem Case Study over Houston

Aerosol-cloud interactions remain a major uncertainty in climate projections for deep convection. Using WRF-Chem with spectral-bin microphysics at 1 km resolution, we simulate a convective event in Houston to investigate aerosol modulations across four anthropogenic emission scaling scenarios: a zero-emission clean background (0x), a reduced-emission case (0.5x), a baseline control (1x), and an enhanced-pollution case (1.5x). Our results show a non-monotonic precipitation response: total storm rainfall peaks at the 1x baseline (+11.5% vs. clean), while the 0.5x scenario exhibits a -3.3% deficit. We attribute this to an “efficiency sweet spot” at moderate loadings, where high warm-phase efficiency leads to premature rainout that depletes the storm’s moisture reservoir. Microphysical analysis confirms a clear Twomey response, inducing warm-rain suppression in the most polluted scenarios (1x and 1.5x). In these cases, the precipitation mass fraction remains below 30% throughout the warm layer, allowing liquid water to be retained through the warm phase rather than rained out. This retention leads to large accumulations of ice mass aloft, with the mean Ice Water Path (IWP) exceeding 1200 g/m2, double that of the clean background. We find that the intensified late-stage storm response is driven by a combination of modest invigoration (~10% increase in updraft velocity) and a dominant dynamical trigger. The sudden melting of the retained ice reservoir generates intense localized cooling that strengthens sub-cloud cold pools and triggers a secondary convective surge. These results argue for tracking individual storm lifecycles to capture how urban emissions reshape convective precipitation.

11:45 a.m.

Sarah Garcia (MS)

Inundation–Desiccation Dynamics Regulate Carbon and Sediment Storage in a Semi-Arid Reservoir System

Reservoirs are globally significant carbon sinks, yet the role of fluctuating water levels in controlling carbon burial and preservation in semi-arid reservoirs remains poorly understood. We investigate how fluctuating base level regulates sediment deposition and organic carbon storage in Elephant Butte Reservoir (New Mexico, USA) using remote sensing, sediment coring, grain-size analysis, and loss-on-ignition measurements. Wetted frequency maps derived from 896 Landsat images (1984 - 2023) show that prolonged drought since 2002 has expanded subaerial delta and floodplain areas at the expense of persistently inundated zones. Subaqueous sediments contain the highest organic matter (OM) concentrations and estimated carbon burial rates (584 - 645 gC/m2yr) during the most recent drought interval), exceeding burial rates predicted from fluvial sediment supply alone and indicating a substantial contribution from in-reservoir primary production. In contrast, crevasse floodplain deposits contain little preserved fine sediment and lower OM content despite direct delivery of suspended sediment during overbank flooding. Trench stratigraphy, cores, and field observations show that bidirectional flow through the crevasse and tie-channel, together with desiccation at the crevasse, promotes repeated mobilization of fine sediment between the floodplain and the Rio Grande, limiting long-term OM preservation. Across the reservoir, OM content increases systematically with inundation frequency, demonstrating that sustained subaqueous conditions are the primary control on carbon preservation. These results indicate that declining reservoir stage may reduce carbon burial efficiency by converting persistently submerged sediments into intermittently exposed environments where stored OM becomes vulnerable to oxidation and reworking.

Lunch

Poster Presentations

Floor 2	Floor 3	Floor 4
1 – 11	12 – 21	22 – 31

1 - Arman Abdipour (PhD)

Meteorological data assimilation for improving air quality modeling with WRF-Chem over the Contiguous U.S. and Texas

Accurate meteorological representation is fundamental to reliable chemical transport modeling, yet how meteorological data assimilation (DA) improvements translate into air quality gains across scales remains an open question. This study evaluates the effect of 3DVAR meteorological DA within WRF-Chem on surface ozone (O3), nitrogen dioxide (NO2), and total oxidant level (OX = O3 + NO2) across CONUS at 12-km and Texas at 4-km resolution, including Houston, Dallas, Austin, and San Antonio, for August 2022. DA substantially improves wind fields, MSLP, and PBL structure: MSLP correlation increases by 25% and RMSE decreases by over 50% over CONUS, while Texas PBLH bias drops from 70 to 7 m. Regional analysis reveals larger improvements in the eastern US and limited responses in terrain-complex western regions. In Houston, DA corrects flow to a realistic sea-breeze circulation, directing Ship Channel emissions into the urban core and yielding the largest NO2 improvement (R: +150%, MB: −55%). Inland cities show city-specific O3 responses, including near-total bias elimination in Austin (−95%) and RMSE reduction in Dallas (−24%). However, DA deepens the negative O3 mean bias over Texas and Houston, exposing residual uncertainties in emissions and chemical boundary conditions. Coherent OX improvements confirm DA primarily modifies oxidant transport rather than photochemical production, highlighting the need for coupled chemical DA to fully constrain surface ozone.

---

2 - Nirvan Abhilash (PhD)

Persistence of Multi-Year La Niña Events: Observational Uncertainty, Subtropical Teleconnections, CMIP6 Model Biases, and Heat Budget Analysis

Multi-year La Niña events strongly influence rainfall, drought, and global climate, yet their persistence mechanisms and model representation remain poorly understood. This study addresses three questions: How consistent are multi-year La Niña signatures across observational datasets? What teleconnection and preconditioning processes sustain them? And how well do CMIP6 models capture these processes? Using seven SST datasets (1900-2025), Year 1 Niño3.4 cooling peaks near -1.3 to -1.4°C, with anomalies frequently extending into Years 2 and 3. Multi-year events sustain stronger zonal SST gradients and reinforce the Walker circulation relative to single-year events, though dataset spread in cooling magnitude underscores observational uncertainty. Negative PMM phases reinforce persistence, while extreme El Niño preconditioning triggers thermocline heat discharge in Type 1 events, and subtropical PMM coupling sustains Type 2 events without a strong precursor. A mixed-layer heat budget using Reynolds decomposition across three ocean reanalyses and four entrainment methods reveals structurally distinct dynamical pathways: Type 2 buildup is dominated by anomalous zonal advection while Type 1 shows partial cancellation between large competing terms. Surface heat flux governs decay timing for both types. Across 46 screened CMIP6 models, with 12 base models and 119 ensemble members analysed in detail, models reproduce single-year events but systematically underestimate two-year and three-year La Niña frequency, reflecting biases in ocean memory and subtropical feedbacks. These findings highlight the need for improved subtropical-tropical coupling in climate models to advance multi-year La Niña prediction.

3 - Jumoke Akinpelu (PhD)

Crustal structure, tectonostratigraphy, and hydrocarbon potential of the deepwater Potiguar Basin, Brazilian Equatorial margin

The Potiguar Basin, located along the Equatorial Margin of northeastern Brazil, is a mature hydrocarbon province with production mainly from onshore and shelfal fields. Despite declining production, recent deepwater exploration has renewed interest in the basin's offshore potential. This study evaluates hydrocarbon prospectivity in underexplored deepwater and ultra-deepwater areas (1,500–2,500 m water depth) through integrated seismic, potential field, geochemical, and 3D basin modeling analyses. More than 11,600 km² of 2D seismic data, complemented by two 3D seismic volumes tied to five wells, were interpreted and integrated with gravity and magnetic data to resolve basin architecture and crustal structure. Results indicate that the Potiguar margin is a highly oblique rifted-passive margin formed in a right-lateral pull-apart setting, with a wide (~220 km) necking zone. Two main syn-rift phases are identified within the Pendência (Late Berriasian–Early Barremian) and Pescada (Late Barremian–Early Aptian) formations, overlain by a thick post-rift sag sequence (Alagamar Formation) and a late passive-margin succession extending from the Upper Cretaceous to Recent. Geochemical data reveal good to excellent source-rock quality across syn-rift, post-rift, and passive-margin intervals. Thermal maturity modeling indicates that Mid-Aptian to Cenomanian source rocks in deep and ultra-deepwater settings are predominantly within the oil window, with modeling suggesting an oil-prone system. Three primary play types are identified: syn-rift structural traps, early post-rift stratigraphic and strike-slip–related traps, and Late Cretaceous turbidite systems. Overall, the study demonstrates a viable and underexplored deepwater exploration fairway in the Potiguar Basin, analogous to productive Equatorial West African margins.

4 - Saad Alabbasi (PhD)

Integrated hyperspectral and aeromagnetic analysis of structural controls on hydrothermal alteration in the Jabal Hamra region, Arabian Shield, Saudi Arabia

The Arabian Shield contains numerous hydrothermal mineral systems related to Neoproterozoic tectonic events and arc terrane development. Structural elements, including faults, shear zones, and fracture networks, generally control the flow of hydrothermal fluids and the formation of alteration zones that may include mineralization. The spatial link between structural architecture and modification distribution is inadequately defined in numerous areas of the shield. This research combines hyperspectral remote sensing with aeromagnetic geophysical data to assess structural influences on hydrothermal alteration in the Jabal Hamra area of northwestern Saudi Arabia. The PRISMA satellite's hyperspectral images was analyzed to detect diagnostic alteration minerals linked to hydrothermal systems. Spectral analysis of the images was conducted to map these minerals. The resultant mineral maps indicate clusters of alteration throughout the research area. Regional aeromagnetic datasets were analyzed to identify structural factors that could influence hydrothermal fluid paths. Magnetic derivatives, such as the tilt derivative and total horizontal gradient, were employed to augment structural lineaments and delineate significant fault systems. The analyzed structural framework indicates many predominant fault orientations going northeast-southwest and northwest-southeast. The combination of hyperspectral alteration maps with aeromagnetic structural analysis reveals a significant spatial correlation between alteration zones and principal structural corridors. Numerous alteration clusters are present at fault junctions and linear structures inferred from magnetic data. These structures presumably functioned as conduits for hydrothermal fluids that facilitated alteration and potential mineralization. Initial field observations and geochemical analysis of the collected rock samples corroborate the existence of hydrothermal alteration assemblages aligned with the remote sensing interpretation. The findings indicate that the combination of hyperspectral mineral mapping with aeromagnetic structural analysis creates an efficient methodology for detecting structurally controlled hydrothermal systems. This methodology provides a scalable framework for regional mineral exploration in the Arabian Shield and may enhance the targeting of hydrothermal mineral resources in Precambrian terranes.

5 - Claudia Aramburu Tinoco (BS)

Monitoring the Spatiotemporal Variability of Suspended Sediment in Texas Bays

Texas coastal wetlands and estuaries provide critical ecological services and protect against storm surges and flooding, yet face increasing stress from sea level rise, subsidence, and sediment supply reduction. Understanding suspended sediment dynamics is crucial for predicting shoreline evolution and long-term coastal resilience. This study investigates spatial and temporal variability in Total Suspended Solids (TSS) in Texas estuarine systems of Trinity and Matagorda Bays, using monthly field campaigns (August 2024 – July 2025) and hyperspectral remote sensing. We collected TSS, particulate organic carbon (POC), salinity and temperature profiles, bathymetry, and reflectance spectra. Hyperspectral imagery enabled improved TSS retrieval compared to conventional multispectral methods by capturing fine spectral variation in complex coastal waters. In-situ measurements reveal significant variability: near a constructed ship channel in Matagorda Bay, TSS concentrations were up to seven times higher than those at the mouth of the Colorado River, suggesting non-fluvial drivers, such as resuspension due to human activity, are important drivers of sediment dynamics in the region. We integrated our dataset with USGS river discharge, NOAA tidal records, and wind data. We found no correlation between river discharge and TSS in either bay, supporting the idea that ship channel activity and other anthropogenic disturbances are likely the primary drivers of sediment suspension in these systems. These findings highlight the growing role of anthropogenic activity in shaping sediment dynamics, directly implying for the management of navigation infrastructure and the design of coastal resilience strategies in Texas wetland systems.

---

6 - Ruth Beltran (PhD)

Three phases of continental rifting of the Early Cretaceous, northern Campos Basin, Brazil

I created a structural restoration and quantitative fault analysis of a 240-km-long, seismic reflection line across the non-volcanic, rifted margin of the northern Campos Basin, Brazil. I used 3D seismic reflection data and well data to constrain the spatial and temporal distribution of strain during the three-phase rifting process: Phase 1 rifting of Early Barremian age, with a regional angular unconformity marking the end of Phase 1 rifting. Phase 2 rifting of Barremian-lower Aptian age mainly from reactivation of Phase 1 normal faults rather than by the formation of new faults. Phase 2 normal faults control 100-800 m-thick deposits in freshwater to brackish lakes, which contain carbonate buildups on structural highs and mudstones in sedimentary depocenters that thicken to 1.4 km to the east. Phase 2 syn-rift sedimentary sections are capped by a 50-100 m-thick Aptian sag sequence. Phase 3 rifting of Late Aptian formed a 60-km-wide, marginal rift filled by volcanic rocks with carbonates on highs within the distal edge of the necking zone. The balanced cross-section shows a cumulative crustal extension of 27 km along the transect. The Phase 3 rifting is followed by a period of erosion before the deposition of the 2-km-thick Aptian evaporite layer. The shift over a time period of 17 myr from more landward, normal faults of Phase 1 to more seaward (Phases 2 and 3) is common among non-volcanic, rifted margins worldwide and provides important insights into the thermal history and hydrocarbon potential of the margin.

7 - Kyra Bennett (MS)

Random Forest classification of California oils using molecular marker ratios

Chemometric methods are increasingly used in petroleum geochemistry to analyze complex molecular datasets for reservoir characterization and oil correlation. Traditional classification relies on expert interpretation of molecular marker ratios from GC-MS data; however, as datasets grow in size and complexity, machine learning approaches offer a more reproducible, multivariate classification. This study applies a Random Forest classifier to the California oil dataset of Peters et al. (2008), which includes 676 oils, tarballs, and seep samples from multiple petroleum systems. Eighteen molecular marker ratios derived from terpanes, steranes, aromatics, and hopanes were used to capture geochemical controls, including depositional environment, source input, and thermal maturity. Samples were classified into petroleum families and tribes following the established framework. Data preprocessing included validation, median imputation, and feature standardization. A stratified 80/20 train-test split was used with hyperparameter optimization via cross-validation. Model performance was evaluated using accuracy and weighted F1 score. The Random Forest model achieved 93% accuracy (weighted F1 = 0.93) in petroleum family classification. Misclassifications occur primarily between closely related Monterey-sourced oil families, while tribe-level classification is highly robust, achieving approximately 99 percent accuracy. Feature importance analysis indicates that tricyclic terpane ratios, sterane parameters, and hopane indices are the most influential predictors, consistent with established geochemical interpretations. Future work will extend this framework using interpretable unsupervised methods such as Self-Organizing Maps.

8 - Jay Braddock (BS)

Trace element geochemistry of olivine in Kainsaz (CO3.2) and Krymka (LL3.2) meteorites show variable moderately volatile element concentrations and extreme reducing environments for inner and outer Solar System materials

Olivine is a common meteorite-building mineral that forms early in the solar system. Its chemical composition is dependent on the formation environment, which have diverse formation conditions that include silicate melt-mineral and vapor-mineral reactions. Primary olivine can record the geochemical conditions of their formation and secondary changes can significantly alter their primary compositions. To assess the variability of moderately volatile element (MVE) concentrations between inner and outer Solar System materials, olivine in carbonaceous and ordinary chondrites Kainsaz and Krymka, respectively, were analyzed for their major and trace element concentrations using laser ablation inductively coupled plasma mass spectrometry (LA-ICP-MS). Olivine shows variable Mg# consistent with the specimens' low petrologic types. Unusually low Fe, Ni, and Co and relatively high MVE composition olivine clasts in Kainsaz point to extreme reducing conditions that resulted in Fe0 (metal) that strongly partitioned the Ni and Co into the metal phase leaving behind Fo(99) olivine. This highly reducing environment was likely a hot hydrogen gas present early in the condensation of the outer Solar System, making these olivines older than the surrounding chondrules. The relatively high abundance of refractory elements in Krymka indicate early condensation in the inner solar system.

9 - Conor Cahill (MS)

Regional evaluation of the distribution and quality of Mesozoic source rocks from the rifted-passive margins of Nova Scotia and Newfoundland-Labrador

Offshore production from the rifted passive margin of Newfoundland and Labrador supplies ~4% of Canada's oil, whereas production offshore of Nova Scotia ended in 2018. These margins formed in different tectonic settings, with Nova Scotia developing during the Late Triassic–Early Jurassic opening of the Central Atlantic Ocean and the northern Newfoundland–Labrador margin forming during the Late Jurassic–Early Cretaceous opening of the Labrador Sea. The primary source rock in Nova Scotia is the Late Jurassic-Early Cretaceous Verrill Canyon Formation, comprising calcareous shales deposited in a restricted-open marine environment. The primary source rock in Newfoundland is the Kimmeridgian Egret Member (Rankin Formation), also calcareous shales deposited under reducing marine conditions. Early Jurassic restricted marine shales (Mohican, Iroquois Formations) represent a secondary Nova Scotia source, likely characterized by Organofacies B; although undrilled offshore, contemporaneous samples from the conjugate Moroccan margin suggest comparable source quality. Here, I have compiled publicly available geochemical data to evaluate the distribution, timing, and quality of select source intervals on both margins. Kinetic modeling following Pepper and Corvi (1995) restores TOC and hydrogen index values to pre-maturation conditions, yielding ultimate expellable potential (UEP) estimates. On both margins, UEP systematically increases basinward; distal settings yield the highest values, suggesting higher prospectivity in the largely unexplored deepwater settings. In Nova Scotia, well J-47 (~216 mmboe/km²) outperforms the more proximal O-76 well (~147 mmboe/km²). Similarly, in Newfoundland, outer-rift well I-78 (~232 mmboe/km², G ~0.30) exceeds inner-rift wells K-55 and P-52 (~115–145 mmboe/km², G ~0.24–0.27).

10 - Ashra Dehghani (BS)

Developing a Triple Oxygen Isotope Record from the Rodrigues Island

The main goal of this project was to demonstrate how triple oxygen isotopes (O16, O17, O18) can be used to determine past fluctuations in climate conditions. Carbonate powders were drilled along the stalagmite growth axis, at intervals of 1—2 mm with a total amount of 120 samples. A microbalance was used to weigh 25-35 µg from each unknown in addition to 20 QA/QC samples. 48 total international carbonate standards (24 IAEA-603 and 24 NBS-18) bracketed the samples during analyses. Each of the weighed samples or standards were placed in Labco exetainers for stable isotope analyses and prepared for laser analysis by having the ambient air flushed using ultrapure N2 gas. Small amounts of acid were injected into each vial to release CO2 gas. This CO2 gas was then analyzed using the Tunable Laser Direct Absorption Spectroscopy (TILDAS) for d18O, d17O, and 17Oexcess values. Preliminary results show that d18O varies between 32.73 and 41.91‰, vs. VSMOW, d17O varies between 21.78 and 17.16 ‰, and 17Oexcess varies between -1187 and 2048 per meg. We note that the rise and fall in d18O values reflect dryer conditions and heavier rainfall, respectively. Rises in 17Oexcess indicate lower relative air humidity derived from oceanic sources. Each of these rises in 17Oexcess is preceded by a drop in d18O, which would suggest an increase in precipitation followed by a subsequent drop in oceanic water derived relative humidity.

11 - Muhammad Nauman Ejaz (PhD)

High-Resolution Seismic Probing the 410 Km Discontinuity Beneath the Sea of Okhotsk

The Sea of Okhotsk, driven by the subduction of the Pacific Plate, is globally renowned for hosting the deepest and largest deep focus earthquakes. Historically, this region was the first where lower mantle slab penetration was observed. Characterized by a steady subduction rate of approximately 4 cm/year, this relatively uncomplicated tectonic regime provides an ideal natural laboratory to investigate the 410 km seismic discontinuity marking the critical mineralogical transition from olivine to wadsleyite. Understanding the structural and thermal evolution of the slab within the Mantle Transition Zone requires precisely imaging the topographic undulations of this phase boundary. However, conventional imaging techniques fundamentally lack the vertical resolution and marine station coverage needed to resolve sharp phase topography. To overcome these limitations, I propose to map high resolution 3D topography of the 410 km discontinuity in this region utilizing pre-stack Kirchhoff migration of source side pP underside reflections. Taking earthquakes deeper than 450 km as bottom-up illuminators, my methodology allows a precise mapping of the geometric variations caused by the cold subducting slab. Following structural imaging, the seismically mapped depth perturbations will be translated into a localized 3D geo-mechanical pressure field relative to the ambient mantle. Finally, these differential pressures are thermodynamically inverted using the Clapeyron slope to extract a quantified thermal profile of the subducting plate. I expect this research to yield new structural and thermodynamic constraints on the 410 km boundary of the region, significantly advancing our understanding of deep slab dynamics and the mechanisms driving deep focus seismicity.

12 - Nilay Gungor (PhD)

Facies Architecture and Depositional Evolution of Plio-Miocene Deep-Water Channel Complexes, Offshore Mahanadi Basin, India

The Mahanadi Basin, located on India's eastern passive margin, contains a Miocene –Pliocene deep-water depositional system that records changes in sediment routing and channel architecture through time. This study integrates 3D seismic interpretation, relative geological time horizon extraction, RGB spectral decomposition, seismic attributes, and well-log calibration to characterize seismic facies, depositional evolution, and reservoir distribution within a high-resolution offshore dataset. Five seismic facies are identified based on reflection amplitude, continuity, and internal geometry, including sheet-like turbidite deposits, channelized fills, mud-dominated slope deposits with polygonal faulting, levee–overbank deposits, and mass-transport deposits. While channelization is limited in older intervals, a well-organized deep-water channel system develops during the Early Miocene, initially sourced from the northwest and expressed as low-sinuosity channels. During the Middle Miocene, an additional sediment input from the northeast is observed, marking a reorganization of sediment routing and the development of more sinuous channel systems. Channel systems evolve into laterally extensive channel–levee complexes, followed by reorganization characterized by avulsion and the development of sediment waves. Channel fills show significant variability, with both sand-prone and mud-prone deposits occurring within the same system. These can be differentiated using seismic amplitude, attribute responses, and compaction signatures. Post-stack seismic inversion is applied to selected channel complexes to evaluate acoustic impedance variability. Overall, the results demonstrate that sediment routing and channel dynamics strongly control facies distribution and reservoir variability in deep-water systems.

13 - Farzina Haque (MS)

Experimental investigations of Ca- and Mg-rich carbonates formation and their isotope fractionations: Constraints on Martian meteorite ALH 84001.

The Martian meteorite ALH84001 has been a subject of extensive debate since the possible existence of ancient Martian life was first proposed. A defining feature of this meteorite is the presence of carbonate globules exhibiting non-equilibrium chemical compositions, characterized by micron-scale zoning with calcium (Ca)-rich cores and magnesium (Mg)-rich rims, along with significant variations in carbon (C) and oxygen (O) isotopic compositions. These carbonates preserve valuable information about the ancient Martian atmosphere and fluid conditions, which can be better understood through experimental replication of their formation processes. In this study, a series of laboratory experiments were conducted to precipitate Ca- and Mg-bearing carbonates under various controlled conditions, including temperature (20 to 120 °C), Mg/Ca ratios (2 to 3), and pCO2. Mineralogical characterizations indicate the formation of Ca-rich and Mg-rich carbonate phases. Carbon and oxygen isotope results show a wide range of $\delta^{13}C$ and $\delta^{18}O$ values under different experimental conditions (temperature, in particular). The fractionations between starting CO2 and carbonate products are not equal to the theoretical equilibrium values, suggesting kinetic isotope effects. These results demonstrate that fluid dynamics and geological conditions play a key role in generating chemical and isotopic variabilities, providing new constraints on the nonequilibrium processes that may have influenced the formation of ALH84001 carbonates.

14 - Ammar Hussain (PhD)

Integrated Hyperspectral Imaging and Geochemical Characterization of LCT Pegmatites Hosting Critical Mineral Deposits in Collision Orogen

Pegmatites in Shigar Valley (Kohistan Island Arc–Eurasian Plate boundary) represent a significant but underexplored source of Li–Cs–Ta (LCT) mineralization in collisional orogenic setting. Hosted within the Dassu Orthogneiss, these sub-horizontal bodies exhibit distinct internal zoning. Their coarse-grained core zones represent significant potential LCT mineralization. A field campaign was conducted across Shigar Valley to investigate the occurrence and evolution of LCT-type mineralization. The pegmatites contain coarse crystals of quartz, feldspar, schorl, muscovite and lepidolite. Laboratory hyperspectral imaging in the VNIR, SWIR, and LWIR ranges were used to identify mineral phases in hand samples. Lithological variations were mapped using PRISMA hyperspectral data and delineate pegmatite zones based on diagnostic absorption features near ~2190–2206 nm and ~2330–2340 nm associated with muscovite and lepidolite. Geochemical results indicate progressive magmatic differentiation. Highly fractionated pegmatites show elevated Rb, Ta, Sn and Li (0.5-2.14 wt%) concentrations. Low Nb/Ta ratios (<0.5) and low K/Rb ratios (<30–100) indicate advanced fractionation consistent with rare-metal–fertile LCT pegmatites. Lepidolite is primary lithium-bearing mineral based on SWIR spectra, while tourmaline indicates boron-bearing magmatic fluids. Samples with elevated Ta but limited Li represent intermediate crystallization stages, reflecting decoupled enrichment of Ta and Li during pegmatite evolution. Feldspar and clay minerals identified in hyperspectral spectra indicate subsolidus hydrothermal alteration caused by late-stage low-temperature fluids. This approach demonstrates that integrated hyperspectral and geochemical analysis is a powerful tool for mapping rare-metal fertile pegmatite systems and constraining their magmatic–hydrothermal evolution in complex orogenic settings.

15 - Onur Karaca (PhD)

A Machine Learning Approach for Estimating Total Suspended Solids in Estuarine Waters Using Hyperspectral Satellite and In Situ Data

Accurate and spatially comprehensive monitoring of Total Suspended Solids (TSS) is essential for understanding sediment dynamics and water quality in estuarine environments. In this study, machine learning models were applied to hyperspectral satellite data to estimate TSS in Matagorda Bay and Trinity Bay, Texas. A total of 117 water samples, collected during monthly field campaigns between August 2024 and July 2025, were used together with hyperspectral reflectance measurements (400–900 nm) to train and validate five models: CatBoost, Random Forest, XGBoost, LightGBM, and Partial Least Squares Regression. Model performance was evaluated using R^2, RMSE, and Taylor diagram analysis. The results indicate that tree-based ensemble models outperformed other approaches, with CatBoost achieving the highest accuracy (test R^2 up to 0.96 and RMSE as low as 8.3 mg L^{-1}). PLSR also showed strong performance as a linear alternative (R^2 up to 0.77, RMSE 11.49 mg L^{-1}). Feature importance analysis suggests that CatBoost's strength arises from its use of informative wavelengths across the full spectrum, with the red region (~630–650 nm) dominating sediment scattering and additional contributions from the blue and NIR regions. The trained models were applied to PRISMA, EMIT, and multi-temporal PACE imagery to produce spatially explicit TSS maps and examine spatiotemporal variability linked to sediment resuspension, hydrologic flushing, and channel–inlet exchange. Overall, CatBoost provided the most consistent results by capturing nonlinear spectral relationships, while PLSR remained effective for representing fundamental sediment–optical interactions.

16 - Haiyang Liao (PhD)

Deep Learning Denoising for Real-Time Dike Intrusion Imaging with Low-Frequency DAS Measurements

Low-frequency distributed acoustic sensing (LFDAS) offers a transformative approach to volcanic monitoring by turning telecommunication fiber-optic cables into dense, high spatiotemporal resolution strainmeter arrays, as demonstrated in tracking dike intrusions near Grindavík, Iceland, at minute timescales. LFDAS requires minimal processing to detect dike intrusion–induced strain, making it particularly attractive for real-time monitoring, early warning, and hazard assessments of volcanic eruptions. However, robust real-time dike inversion remains a challenge due to various noise sources. Long-period laser drift artifacts, impulsive high-frequency disturbances, and complex background noise reduce data fidelity, obscure subtle strain signatures, and directly limit inversion accuracy. Existing noise mitigation methods, such as median filtering and Gaussian process removal, are often computationally expensive, hindering real-time use, and can risk distorting key signals. To address these limitations, we propose a supervised deep learning network trained on synthetic fiber strain-rate datasets to simulate strain-rate responses to dike openings as clean labels, with realistic noise added to create training pairs. We adopt a U-Net trained end-to-end on synthetic clean-noisy strain-rate pairs to directly regress the denoised signal. Preliminary results show effective suppression of long-period and spiky noise while preserving subtle strain features and maintaining computational efficiency, thereby improving dike inversion accuracy. Notably, the denoised data revealed a previously undetected small intrusion event on November 27, 2023, which remains ambiguous after conventional processing. These results underscore the potential of deep-learning-enhanced LFDAS as a high-resolution, real-time tool for imaging subsurface deformations in active volcanic regions, strengthening early warning and hazard assessment capabilities.

17 - Cristina Lyon (BS)

The recorded relationship between a tie-channel and its floodplain

Sediment transport at Elephant Butte Reservoir (EBR) in New Mexico is strongly influenced by summer monsoons and associated flooding. EBR lies within a semi-arid region currently experiencing decadal drought, and what once functioned as a reservoir basin during wet years now hosts an active floodplain and a prograding delta. During flooding events, the Rio Grande delivers high sediment loads, depositing sediment and organic matter across the floodplain. These events may be preserved as stratigraphic packages that record bi-directional flow within crevasse splays. Sediment transfer from the channel to the floodplain is more frequently preserved than the inverse and resulting erosion surfaces are typically abrupt rather than gradational. I hypothesize that the crevasse splay becomes channelized during high-stage river levels and flooding events. To investigate this, I analyzed four L-shaped trenches excavated within a crevasse splay at 10-meter intervals into the floodplain. These exposures reveal evidence of bi-directional flow and variable depositional conditions. Combined with Landsat imagery and wetted-frequency maps, these observations allow for quantification of floodplain evolution in semi-arid reservoir systems and provide insight into how sedimentation patterns respond to drought, monsoon-driven floods, and delta progradation.

18 - Daniel Maya (PhD)

3D basin-scale petroleum system analysis of thermal maturity, expulsion, and migration along Uruguay's deepwater rifted-passive margin

The Early Cretaceous volcanic-rifted margin of Uruguay features 1- 4.5 km-thick basalts (seaward-dipping reflectors, SDRs) filling syn-rift half-grabens (Hauterivian-Barremian, 132-126 Ma). Overlying these SDRs are organic- rich Aptian rocks (122-113 Ma). On the Namibian margin, 14 BBOE of hydrocarbon reserves were found at water depths of 1200-3200 m. This study used 6294 km of 2D seismic data, 22,984 km² of 3D seismic data, and deepwater well data from Uruguay (3 wells), Namibia (5 wells), and the South Atlantic (6 wells). These wells identified three source rock intervals: 1) Post-rift lower Aptian (122 Ma, OAE- 1 A), 2) Upper Aptian (113 Ma, OAE-1 B), and 3) Cenomanian-Turonian (95-93 Ma, OAE II). Similar geochemical signatures in South Atlantic wells suggest that Uruguay's deepwater margin should host these source-rock intervals. A regional 3D basin model covering 95,640 km² incorporated maturity, biostratigraphy, hydrocarbon generation, and expulsion data, producing paleobathymetric and UEP maps correlating source rock quality with subsidence. Using multi-seismic attribute analysis, source rock responses were identified with low acoustic impedance, high reflectivity, and a 10 Hz frequency band, indicating the presence of source rocks in Namibia during the lower Aptian (122 Ma), upper Aptian (113 Ma), and Cenomanian- Turonian (95-93 Ma). Modeled results show an average oil expulsion of acme 122 Ma (41. 48 MMboe/km ²), acme 113 Ma (4. 93 MMboe/km ²), and acme 95-93 Ma (1. 05 MMboe/km ²), high maturity and vertical migration confirmed by the Raya-1x well including heavy gases associated with a deeper Cretaceous thermogenic petroleum system.

19 - Matthew McAllen (PhD)

Regional Crustal Structure and Aptian Source Rock Characterization of the Foz do Amazonas Basin, Brazilian Equatorial Margin

The Foz do Amazonas ("Mouth of the Amazon River") Basin of the Brazilian Equatorial Margin (BEM) is chararacterizd by the deposition of the 5-10-km-thick, late Miocene to Recent Amazon delta or cone being deposited on thinned continental crust and the adjacent oceanic crust of Aptian-Albian age. Previous petroleum exploration of the Foz do Amazonas dates to the 1970s and 1980s and includes 95 wells drilled mainly on the shelf and upper slope with only ten wells with hydrocarbon shows and none resulting in commercial production. In this study, I describe results in three areas: 1) I use gravity data in the Foz do Amazonas to define the continent-ocean boundary (COB); the oblique rifts across a narrow, necking zone of thinned, continental crust; and the doughnut gravity signature that reflects the flexure of the crustal substrate related to the load of the Amazon delta; 2) I created burial plots based on wells in the lower slope and deepwater area along with temperature data to define the oil and gas windows with emphasis on the outer doughnut area where Aptian source rocks on both thinned, continental crust and oceanic crust have remained in the oil window; 3) I use publicly available, geochemical data to estimate the Ultimate Expellable Potential (UEP) of the Aptian source rock intervals that show that expellable potential is highly variable in the basin, with 1APS-0029-AP yielding 14 mmboe/km2 of oil and the 1APS-0018-AP yielding 116 mmboe/km2.

20 - Zohaib Naseer (PhD)

Data-Driven Geothermal Prospectivity Mapping of Sandstone Reservoirs Using Multi-Geophysical Datasets and Machine Learning: A Case Study of Thar Platform, Lower Indus Basin, Pakistan

The emerging techniques in renewable energy resources are advancing worldwide. There are various sustainable energy resources, such as wind energy, solar energy, and hydro power. Besides these resources, geothermal energy is a vital source of subsurface heat generated within the Earth, due to its eco-friendly nature and increasing global demand. Current studies are based on a comprehensive analysis of geothermal resources using geophysical techniques, including petrophysics, gravity and seismic, methods, which are applied to the sedimentary basin of Pakistan. A regional-scale analysis is performed using gravity data, with detailed mapping of Bouguer anomalies to understand variations in subsurface density. and dip estimation by using digital elevation model map. Following regional studies, seismic data interpretation is conducted to determine subsurface structural geometry, as trapping structures play a crucial role in fluid accumulation beneath the surface. For geothermal exploration, structures with normal faulting, especially horst and graben geometry, are considered ideal for fluid accumulation with geothermal potential. The primary goal of this study is to identify petrophysical and thermal parameters of the subsurface lithology to locate zones with potential for geothermal fluid accumulation and facies analysis. Petrophysical properties such as shale volume, porosity, and permeability are critical because fluid storage depends on pore spaces and their interconnectivity. In addition to petrophysical parameters, thermal properties like formation temperature, geothermal gradient, heat production, and radiogenic heat output provide direct information about subsurface heat. These results are later correlated with core data and well production reports for calibration and validation. Furthermore, evaluating surface structural trends and deformation patterns using DEM-derived dip analysis in order to identify fault-controlled zones that may enhance geothermal fluid circulation and delineation of subsurface density variations using Bouguer anomaly mapping and assess their relationship with basement configuration, heat sources, and structural controls relevant to geothermal resource potential is also a part of this study. The findings indicate that the target formation (Lower Goru Formation) contains interbeds of sandstone and shale, which act as excellent thermal traps for geothermal energy. These diverse techniques show that sedimentary basins, often overlooked, can lack viable geothermal resources, contributing to clean energy transitions in tectonically active and developing regions. The outcomes are expected to support sustainable geothermal development strategies and encourage policy-driven investment in renewable energy infrastructure.

21 - Pauline Nguyen (BS)

Assessing Organic Carbon Pools in Coastal Prairie Soils

Coastal prairie soils are a potentially important component of regional carbon storage. To evaluate carbon quantity and stability, 35 topsoil and subsoil samples from remnant and restored prairies at the University of Houston Coastal Center were analyzed using Rock-Eval 6 programmed pyrolysis. Results showed spatial and ecological differences in quantity and durability of soil organic carbon. Measured total organic carbon ranged from 0.16% to 4.05%, indicating substantial heterogeneity across sites and depths. S1 values (0.02–0.13 mg/g) reflected small pools of thermally labile organic matter, while S2 values (0.17–6.63 mg/g) revealed greater variability in more thermally stable carbon compounds. Remnant prairies consistently exhibited higher TOC concentrations and a greater proportion of stable carbon, expressed as S2/(S1+S2), than restored prairies, suggesting that ecosystem maturity and lower disturbance favor carbon preservation. Model outputs further supported these trends, identifying remnant prairies and topsoils as having the greatest potential for long-term carbon storage. ANOVA statistical analysis reinforced that both management history and soil depth significantly influence carbon abundance and stability. Carbon content and thermal stability declined with depth, indicating that topsoil functions as the dominant long-term carbon reservoir in these systems. Overall findings show that remnant coastal prairies store more carbon and a more stable form of carbon than restored sites, highlighting the importance of ecosystem history, management, and depth in controlling soil carbon stabilization. Finally, PARTYSOC machine-learning model was used to assessed proportions of centennially labile and stable soil organic carbon.

22 - Oriyomi Ojelabi (PhD)

LIDAR, GPR, and seismic investigation of aplite dikes and exfoliation at Enchanted Rock, Texas

Enchanted Rock, a prominent granite batholith in Central Texas, is known for its unique geological features, including its smooth surface, exfoliation layers, erosional depressions, vernal pools, and aplite dikes. The aplite dikes are integral to the petrologic and structural evolution of plutonic bodies; however, their internal geometry remains poorly understood. This study uses drone photogrammetry and airborne LIDAR data to establish the detailed topography of the exposed dome. In addition, we have undertaken 2D seismic surveys over parts of the dome and have some evidence of reflections from possible deep (>50 m) layers as well as the dikes. We have also employed a Sensors & Software Noggin 250 MHz SmartCart ground penetrating radar (GPR) system to image the subsurface geometry of aplite dikes within the exposed granite dome. The high dielectric properties of the granite at Enchanted Rock enhance GPR signal resolution and depth penetration. Data were collected to a depth of approximately 10m across a 10 × 50 m grid with 1-meter line spacing. Fifty-one GPR profiles were collected in the north-south direction and eleven in the east-west direction. Additional transects were conducted from the base to the summit of the dome and back, as well as along areas with visible aplite dike exposures. In several profiles, aplite dikes are observed as continuous, gently dipping events with some hyperbolic scattering at intermediate depths. These reflections correlate with surface-exposed dikes and are interpreted as subsurface extensions of the aplite intrusions. Our findings contribute to the understanding of batholiths and exfoliation domes.

23 - Estefani Ruiz Toro (MS)

The tectonic role of the Bering Sea oceanic plateau in the Great Northern Pacific Plate Reorganization

The political division of the northern Pacific plate margin between northeastern Asia in Russia, the Bering Sea, and Alaska and the Aleutian Islands in the USA has slowed the tectonic understanding of this vast, 9.1 million km² region. In this study, I have compiled geologic, gravity, magnetic, seismic reflection, well logs, heat flow, and radiometric data from on-land and submarine crustal provinces of Russia and the USA to define the progressive, Cretaceous-Cenozoic collisional events that have shaped the northern margin of the Pacific Plate. These crustal provinces include: 1) Precambrian cratons of northeast Russia and Alaska that act as continental backstops; 2) the Cretaceous (96-67 Ma) Okhotsk Andean-style arc that formed along the southern edge of the craton, and its southward-facing accretionary belt which can be traced from Russia into the southern, accreted terranes of Alaska; 3) the Paleogene (55-44 Ma) Olyutorsky intraoceanic arc that can be traced from Kamchatka along the northern and eastern margins of the Bering Sea; 4) the Cretaceous-Eocene (75-44 Ma) Bering oceanic plateau with a 13-17-km-thick crust that collided with Russia at the Koryak Range, terminated magmatism along the Olyutorsky arc at 44 Ma, indented the Alaskan margin along the right-lateral East Bering Sea fault zone, and resulted in a 1,200-km southward migration of the plate boundary to the presently active Aleutian volcanic arc. I attribute the prominent bend in the Hawaiian-Emperor seamount chain at 44 Ma to a major change in Pacific plate motion triggered by the accretion of the Olyutorsky arc and Bering oceanic plateau.

24 - Celine Saidy (MS)

Mapping Vegetation and Erosion Change at Natural and Restored Dunes on Texas Barrier Islands

Sand dunes are a key feature of Texas's barrier islands. They provide protection from erosion and flooding, as well as host a vibrant ecosystem. However, a combination of anthropogenic development and intensified storm activity in the Gulf is increasingly degrading dunes on the barrier islands along the Texas Coast. A wide variety of restoration methods have been tested and employed, most of which involve introducing vegetation by planting robust native species. Despite this, it is still difficult to restore degraded dunes to the full resilience and ecological functionality of a natural dune. However, a comparative study of natural and restored dunes is lacking. The study will use drone-based multispectral imagery and LiDAR data collected from six sites along the Texas coast in May 2024, July 2024, and June 2025 to visualize changes in vegetation and elevation at a number of sites, with some consisting of natural dunes and some consisting of restored dunes. Prominent vegetation species at each site will also be considered in the analysis.

25 - Bilge Sasmaz (MS)

Development of a 1D Mechanical Earth Model and Fracture Analysis at the HFTS-1 Site, Midland Basin

Unconventional reservoirs such as the Wolfcamp Shale in the Permian Basin are characterized by low permeability and therefore require hydraulic fracturing to achieve economic hydrocarbon production. Designing effective hydraulic fracture treatments necessitates an accurate understanding of pore pressure and in-situ stress conditions. Two principal methods are currently used for estimating in-situ stresses: the poroelastic approach and the viscoelastic stress relaxation model. In this study, these two approaches will be compared using an extensive set of data acquired as part of a large field-based R&D project funded by the US Department of Energy and the Exploration and Production Industry at Hydraulic Fracture Test Site 1 (HFTS-1), located in the Midland Basin, Reagan County, Texas. The Wolfcamp Formation exhibits significant lithological variability, particularly between carbonate-rich and clay-rich intervals. This variability leads to notable stress variations with depth, which have important implications for hydraulic fracture propagation.The minimum horizontal stress will be computed using the poroelastic approach, calibrated with measured fracture closure and reopening pressures obtained from Modular Formation Tests (MDT). Each modeling approach will then be used to construct a one-dimensional Mechanical Earth Model (MEM). A MEM integrates well logs, image logs, and stress data to characterize the subsurface mechanical properties and fracture responses under varying stress conditions. It allows stress distribution and rock failure mechanisms for the various stratigraphic units to be predicted. The MEMs offer the required geomechanical framework to support hydraulic fracture design, wellbore stability, low-frequency DAS monitoring responses, and reservoir performance evaluation. The two modeling approaches will then be compared with available hydraulic fracture and microseismic data to assess their predictive capabilities and practical implications. This comparison is expected to provide valuable recommendations for optimized fracture modeling and reservoir development strategies in unconventional reservoirs.

26 - Md Upal Shahriar (PhD)

Structural and Stratigraphic Characterization of the Andaman Fore-Arc Basin: Implications for Hydrocarbon Prospectivity

The Andaman fore-arc basin, located in one of the world's most tectonically complex regions, has undergone extensive hydrocarbon exploration since the 1990s, with limited success. Formed by the collision of the Indian and Burma plates, the basin experienced compression and downward folding during accretionary prism emplacement, followed by strike-slip movement driven by the oblique subduction of the Indian oceanic plate. This study integrates 2,351 km² of 3D seismic data and well logs from five wells to decode the basin's structural and stratigraphic framework and assess its hydrocarbon exploration potential. Seismic mapping, well correlation, and attribute analysis — including outcrop, coherence, sweetness, and post-stack inversion — were used to characterize sand, channel complexes, mass transport deposits (MTDs) and volcanics. The structural and stratigraphic analysis reveals a well-defined petroleum system within the Andaman fore-arc. The basement exhibits normal faults inherited from the pre-existing Burma plate configuration, over which large volumes of sediment accumulated. Oligocene syn-tectonic depositions contain thick sequences of organic-rich shales and mudstones confirmed as the primary source rock through sweetness attribute analysis, alongside significant volcanic activity. During the Miocene, limestone depositions were recorded alongside major sandstone reservoir development, which continued into the Pliocene. Stacked channel systems served as conduits for large submarine fan complexes during the Miocene and Early Pliocene, while canyon systems along the eastern fore-arc contributed to significant MTD accumulations. Trapping is predominantly stratigraphic, controlled by pinch-outs, with subsidiary four-way and three-way structural closures. Together, these elements define a credible and mappable petroleum system with meaningful exploration targets. This study presents the first comprehensive integrated petroleum system analysis of the Andaman Fore-arc Basin, offering new insight into its geological complexity and hydrocarbon prospectivity.

27 - Rajesh Silwal (PhD)

Integrating InSAR and Channel Steepness for AI-Based Coseismic Landslide Modeling in the Nepal Himalaya

Earthquake-induced landslides in active orogens such as the Nepal Himalaya pose severe threats to lives, infrastructure, and post-disaster recovery. While machine learning (ML) and deep learning (DL) approaches to coseismic landslide susceptibility mapping have advanced considerably, spaceborne interferometric synthetic aperture radar (InSAR) products, particularly line-of-sight (LOS) displacement and coherence-based damage proxy maps , remain underutilized in event-based frameworks. This study develops a multi-factor coseismic landslide probability model integrating InSAR-derived deformation metrics with geomorphic and hydrologic predictors for rapid post-earthquake hazard assessment. Using the 25 April 2015 Mw 7.8 Gorkha earthquake, LOS displacement was derived from ALOS-2 PALSAR-2 ScanSAR interferometry and the normalized channel steepness index (Ksn) was computed from a DEM. Fourteen conditioning factors trained five architectures: Random Forest (RF), XGBoost, CNN, U-Net, and DeepLabV3 evaluated via leave-one-basin-out three-fold spatial cross-validation on a 655,360-pixel domain (positive-class prevalence 6.35%; no-skill AUC-PR baseline 0.0635). InSAR integration improved AUC-PR across all models by 7.8–17.3%. RF achieved the highest AUC-PR (0.7940; ~12.5× baseline) and CSI (0.3027), balancing landslide recall (88.09%) with specificity (88.68%). XGBoost attained the highest AUC-ROC (0.9501) but showed lower recall and poorer calibration (Brier = 0.1397). Among DL models, DeepLabV3 produced the best-calibrated probabilities (Brier = 0.0693), while CNN achieved the highest recall (92.40%) at the cost of elevated false alarms. Permutation importance identified Ksn as the dominant predictor, underscoring tectono-geomorphic control on landslide occurrence. These findings demonstrate that InSAR integration substantially enhances coseismic landslide hazard assessment and rapid response capacity.

28 - Joshua Tannous (MS)

Barringer Hill and the depositional pattern of llano uplift pegmatite

In the late 19th century America's largest source of rare earth minerals at the time was the Barringer Hill Mine found east of Llano Texas. Early lamp filaments used Ytrium, a metallic rare earth element that was mined at Barringer Hill, but with the invention of tungsten filament bulbs and lamps in the early 20th rendered these early lamps obsolete and led to the closure of the mine and it's eventual damming and submersion under Lake Buchanan. In our current age the rush for rare earth mineral exploration is dominating research and economic interests, for this first semester of my masters program I am integrating Lidar, satellite hyperspectral, and historical geologic data to better understand the trends of pegmatite deposition in the Lake Buchanan area if any such trend exists. I will then use insights gained from this integrated study to select sites for future field work.

29 - Madeline Tompson (BS)

An Analog Experiment to Trace d18O and d13C Evolution Along an Epikarst Flow Path

Stalagmites are excellent paleoclimate archives. An important consideration for their interpretation includes the processes controlling the δ13C and δ18O when waters percolate down to the cave. In open system conditions, water exchanges with air and surrounding bedrock, whereas in closed system conditions, the exchange is minimal to none. Here, we examine how synthetic carbonate δ13C and δ18O signals vary along the flow path. Supersaturated solutions were prepared to flow from source bags through tubes onto watch glasses, imitating stalagmite growth. Carbonate precipitates were collected from the source bags, necks, tube interiors, and watch glasses, and were analyzed for stable isotopes using Isotope Ratio Mass Spectrometry (IRMS) and/or Tunable Infrared Laser Absorption Spectrometry (TILDAS). Results show that both δ18O and δ13C remained relatively stable throughout the tubes, likely due to limited evaporation and CO2 degassing, reflecting the closed conditions under which the experiments were done. The strongest increases of both stable isotopes occur at the watch glass where CO2 degassing was the greatest. The variability of δ13C and δ18O results suggest that there are in-cave processes that control isotopic evolution. Plans to improve this cave-analog experiment will include the usage of carbonate rock and a cross-comparison with an analog under open system condition.

30 - Minh Nhat Tran (PhD)

Strain–based full waveform inversion with automatic differentiation for distributed acoustic sensing.

Distributed Acoustic Sensing (DAS) records strain rather than particle velocity, creating a mismatch with conventional full waveform inversion (FWI) solvers. This study introduces a velocity-strain staggered-grid finite-difference solver to directly simulate strain and enable FWI using DAS data. Automatic differentiation is used to efficiently compute gradients, avoiding complex adjoint derivations. The forward solver is validated against SPECFEM2D and the inversion is tested on synthetic Marmousi data. Results show effective reconstruction of near-surface shear-wave velocity structures, providing a practical framework for DAS-based FWI.

31 - Muhammad Younas (PhD)

Integrated remote sensing and geospatial techniques to characterize the subsidence: A case study of the Texas Gulf Coast, United States

In rapidly increasing coastal regions, identifying the key drivers of land subsidence is crucial for managing groundwater resources, preventing flooding, and maintaining infrastructure. Deep learning and other data-driven approaches offer a useful framework for assessing the relative impact of various anthropogenic and environmental factors on subsidence processes. In this study, Interferometric Synthetic Aperture Radar (InSAR) measurements were combined with the geospatial deep learning model to determine impervious surface dynamics and land subsidence over 300,000 square kilometers in fifty-six counties along the Texas Gulf Coast, from Louisiana to the Mexican border, between 2016 and 2023. Results reveal that in Harris County, subsidence rates reached -3.75 centimeters per year, particularly affecting the northwest and southeast regions. The deep learning model showed significant changes that impact flooding and aquifer replenishment. Over the past two decades, both groundwater and surface water use have been high, with a severe drought from 2011 to 2013 worsening these issues. Our multiple linear regression analysis suggests that population growth (R^2=0.99) and land compaction (R^2=0.98) are key factors in subsidence, along with declining oil and gas production. In Waller County, subsidence rates reached -4.55 cm per year, with similar rates in Chambers County (-3 cm), Karnes County (-2.12 cm), and DeWitt County (-3.83 cm), especially near oil and gas fields. Karnes County faced a drought from 2006 to 2014, coupled with increased water extraction. Linear regression analysis indicate that population growth and groundwater withdrawal significantly contribute to subsidence in these areas. Hidalgo County experiences subsidence rates of up to -1.78 cm per year, particularly in the McAllen Ranch area. The county faced drought from 2011 to 2014, and while population growth and groundwater use contribute to subsidence, recent oil extraction may also play a role.

Keynote Speaker

Dr. Kunxiaojia (Tammy) Yuan

Global Wetland Methane Emissions: From Science to Solutions

3:00 – 3:25 p.m.

2026 Outstanding EAS Alumnus

Dr. Don Van Nieuwenhuise

EAS MS in 1977, EAS Faculty Director and Instructional Professor (2002-2025)

- 1971-1973: Undergraduate in geology, University of South Carolina, Senior thesis on benthic fauna in Puerto Rico
- 1973-1977: MS student at the University of Houston: MS thesis on the impacts of diverting the Santee River in South Carolina
- 1978: PhD student at the University of South Carolina: PhD dissertation on the Black Mingo Formation in South Carolina
- 1978-1981: Exploration geologist, Mobil Corporation in New Orleans
- 1980-1981: Adjunct Professor, Tulane University in New Orleans
- 1981-1986: Senior Research Scientist, Amoco Research Center, Tulsa, Oklahoma
- 1986-1999: Regional stratigrapher and researcher at Amoco in Houston and Stavanger, Norway
- 1999-2001: Research scientist, Energy & Geoscience Institute, University of Utah
- 2002-2025: EAS faculty director and instructional professor, petroleum geoscience programs, University of Houston

Thank You

Thank you to all the volunteers who have assisted with set up and take down. This would not have been possible without you!

The organizing committee would like to thank Edgar Moreno for constructing this year's brochure.

Industry Judges

Francisco Bolivar
Chuck Caughey
Beata Czader
Catherine Donohue
Vsevolod Egorov
Ebrahim Eslami
Igor Faoro
Adam Goss
Ken Green
Fiona Jiang
Katarina Jonke
Bruna Lyra
Sumit Mukherjee
Vincent Polignano
Franklin Ruiz
Bhavik Shah
Abhilash Srungarapati
Madeline Statkewicz
Ana Vielma
Zhefeng Wei
Shawn Wright

UH Faculty

Brandee Carlson
Pete Copland
Sharon Cornelius
Jose Gorosabel
A K M Nahid Hasan
Jinping Hu
Jin Park
William Sager
Jinny Sisson
Ny Riavo Voarintsoa
Tianfan Yan
Honghai Zhang

SRD Organizing Committee

Amberlee Enger
Brandee Carlson
Paul Mann
Antonious Douglas
Jay Krishnan

We would also like to thank and acknowledge the College of Natural Sciences and Mathematics for their contributions. Thank you for your support!

Who Are We?

The Department of Earth and Atmospheric Sciences at the University of Houston has a wide range of research programs central to the earth sciences.

Air Pollution
Air Quality
Applied Geophysics
Applied Rock Physics
Atmospheric Science
Carbonate Petrology
Climatology
Geodynamics
GIS
Hydrology
Igneous Petrology
Inorganic Geochemistry
Isotope Geochemistry
Marine Geology
Micropaleontology
Petroleum Geology
Potential Fields
Remote Sensing
Sedimentology
Seismology
Sequency Stratigraphy
Structural Geology
Tectonics
Thermochronology
Whole Earth Geophysics

The Department offers M.S. and Ph.D. degrees in Geology, Geophysics, and Atmospheric Sciences, B.S. degrees in Geology, Geophysics, Environmental Sciences, and Atmospheric Sciences, and a B.A. in Earth Sciences. Fieldwork is a major component of all degree programs. The Department also offers Professional M.S. programs in Petroleum Geology and Petroleum Geophysics that are offered at convenient hours for professional geoscientists working in industry or aspiring for a professional position within the petroleum industry.

CONTACT US

Department of Earth and Atmospheric Sciences
4800 Cullen Boulevard, Houston, TX, 77204
Phone: (713) 743-3399
Web: http://www.eas.uh.edu

Scan the QR code to sign up for the EAS newsletter!

In Memoriam

Rosalie Frances Maddocks

Professor in Earth and Atmospheric Sciences

1938 – 2026

Rosalie Maddocks dedicated her career to the University of Houston's Department of Earth and Atmospheric Sciences, where her expertise in ostracod taxonomy and systematics, marine micropaleontology, paleobiology, and paleoecology earned her international recognition. A gifted and very passionate educator, she taught oceanography and paleobiology with an intense enthusiasm that left a lasting impression on every student who passed through her classroom. She had a gift for turning careful observation into good science, often encouraging her students to slow down and look closer, reminding them to "put a hand lens on it" when studying fossil identification. Her contributions to this department, to her field, and to the students she taught are immeasurable, and so enduring that no hand lens is needed to see them. She will be remembered with deep gratitude and admiration. In her honor, an endowment has been established to support graduate students in the Department of Earth and Atmospheric Sciences. If you would like to carry her legacy forward, please consider contributing by scanning the QR code.